Chem. Pap. (2017) 71:2195–2208
DOI 10.1007/s11696-017-0213-9

ORIGINAL PAPER

Synthesis, characterization, antimicrobial evaluation and QSAR studies of organotin(IV) complexes of Schiff base ligands of 2-amino-6-substituted benzothiazole derivatives

Aarti Ahlawat[1] · Vikramjeet Singh[2] · Sonika Asija[1]

Received: 8 December 2016 / Accepted: 25 May 2017 / Published online: 6 June 2017

Abstract A series of organotin(IV) complexes of type R_2SnLCl [R = Ph, Bu, Et, Me] were prepared by reaction of diorganotindichloride(IV) with Schiff base ligands, L_1 = (1-[(6-ethoxy-benzothiazol-2-ylimino)-methyl]-naphthalen-2-ol), L_2 = (1-[(6-nitro-benzothiazol-2-ylimino)-methyl]-naphthalen-2-ol), L_3 = (1-[(6-methoxy-benzothiazol-2-ylimino)-methyl]-naphthalen-2-ol) and L_4 = (1-[(6-methyl-benzothiazol-2-ylimino)-methyl]-naphthalen-2-ol) obtained from 2-amino-6-substituted benzothiazole derivatives with 2-hydroxy-1-naphthaldehyde in 1:1 molar ratio. These organotin(IV) complexes were characterized by various spectroscopic techniques (^{1}H, ^{13}C and ^{119}Sn NMR, FT-IR), and physical techniques (X-ray powder diffraction analysis and elemental analysis). The coordination of the prepared complexes has been planned as pentacoordinated around the central tin atom during which ligands coordinated to tin atom in bidentate manner acted as N, O donor system. The ligands and their complexes were screened for antibacterial and antifungal activities against Gram-positive bacteria *Bacillus cereus* (MTCC 10072), *Staphylococcus aureus* (NCIM 2901), Gram-negative bacteria *Escherichia coli* (MTCC 732), *Pseudomonas aeruginosa* (MTCC 424) and fungi *Aspergillus niger* (MTCC 9933) and *Aspergillus flavus* (ATCC 76801). The output of QSAR analysis indicated that topological parameters (molecular connectivity indices) were responsible for controlling the antimicrobial activity of the synthesized compounds.

Keywords Schiff base ligands · Organotin(IV) complexes · Benzothiazole derivatives · Antimicrobial activity · QSAR studies

Introduction

The tremendous rise in non-responsiveness of microorganisms due to widespread increase in resistance to numerous antibiotics is leading to decline in the effectivity of treatments (Hong et al. 2010; Braunstein and Morise 2000). Therefore, the sole recognition to overcome this exigency is effective treatment and implementation of improved drugs (Elebier et al. 2007) which boosts researchers to produce novel drugs by small microorganism variance. The Schiff bases play key role in the development of coordination chemistry to create stable complexes having biological activity, especially chemotherapeutic, antineoplastic, antiproliferative and anti-insecticidal activities (Basu et al. 2012; Mun et al. 2012; Silva et al. 2011). Schiff bases show remarkable research in medicinal, industrial, agricultural and biological fields and have proved effectiveness as catalysts, optical sensors, engineering fields and magnetic materials (Kemmer et al. 2000; Ekennia et al. 2015). The growing interest in the elaborated studies of the coordination chemistry of the organotin compounds of the Schiff bases has been widely explored due to their versatile applications resultant of their physical, chemical and biological properties (Baul et al. 2008; Yin and Chen 2006; Yenisehirli et al. 2010). The structural

Electronic supplementary material The online version of this article (doi:10.1007/s11696-017-0213-9) contains supplementary material, which is available to authorized users.

✉ Sonika Asija
sc_ic2001@yahoo.co.in

[1] Department of Chemistry, G. J. University of Science and Technology, Hisar, Haryana 125001, India

[2] Department of Pharmaceutical Sciences, G. J. University of Science and Technology, Hisar, Haryana 125001, India

elucidations of the organotin complexes have evolved as a subject of attention with commercial applicability in view of their prospective activities (Beltran et al. 2007; Nath et al. 1997; Aman and Matela 2013). Organotin complexes with Schiff bases of benzothiazole derivatives have been extensively studied with specific interest as a result of various applications as antioxidants, antibiotics, herbicides and benzothiazole derivatives also act as flavouring agents and as bioluminescence for fire flies (Devi et al. 2012). Furthermore, they are having broad applications as yellow dyes, pigments and are generally used as intermediates within the preparation of a large variety of biologically vital compounds and as precursors of prospective anti-diabetic drugs (Dias et al. 2015; Nath et al. 2009). The substitution with the heterocyclic system provides potent pharmacological properties such as antihelmintic, anti-inflammatory and analgesic as compared to the standard drugs (Gill et al. 2015, Mene and Kale 2016) and heterocyclic chemistry of substituted benzothiazole derivatives become the most prolific area of interest in drug discovery and development due to increasing importance in pharmaceuticals (Sharma et al. 2017).

In pursuit of all the above facts, the present study focused on the synthesis, spectroscopic analysis, antimicrobial evaluation and QSAR studies of Schiff bases of 2-amino-6-substituted benzothiazole derivatives and their respective organotin(IV) complexes.

Experimental

Materials

All the chemicals (2-hydroxy-1-naphthaldehyde, 2-amino-6-nitrobenzothiazole, 2-amino-6-ethoxybenzothiazole, 2-amino-6-methoxybenzothiazole, 2-amino-6-methylbenzothiazole, dimethyltindichloride, diethyltindichloride, dibutyltindichloride and diphenyltindichloride) were purchased from Sigma-Aldrich and were used without further purification. All the solvents were of analytical grade received from Sigma-Aldrich and used after drying with standard procedures.

Instrumentation

The NMR spectra of the compounds were recorded on 400 MHz using Bruker Avance II 400 MHz NMR spectrometer. The ^{1}H, ^{13}C NMR and ^{119}Sn NMR were recorded using tetramethylsilane and tetramethyltin, respectively, as internal standard in DMSO-d_6. The IR spectra were recorded with samples pressed with KBr pellets using a Shimadzu IR affinity-I 8000 FT-IR spectrometer in the range 4000–400 cm^{-1}. Tin was gravimetrically estimated as SnO_2 after decomposition with concentrated HNO_3 (Sonika et al. 1994). The melting points were recorded on electrical heating coil apparatus and were uncorrected. The X-ray powder diffraction analysis was recorded using Rigaku table top X-ray diffractometer with the scan rate of 2 min in the range 20–80° and the average crystallite size was calculated to acquire impending regarding propulsive of the compounds. The elemental analysis of the compounds was done using Perkin Elmer 2400 instrument. The molar conductance was measured using Systronics conductivity 52 bridge model-306 in DMSO.

The synthesized samples were screened for in vitro antimicrobial activity against bacterial and fungal strains using serial dilution method to evaluate their minimum inhibitory concentration (Spooner and Sykes 1972). The nutrient broth and Sabouraud dextrose broth were used as growth media for bacteria and fungi, respectively, and test tubes having 1 mL of nutrient medium were autoclaved for 30 min at 121 °C. The stock solutions of test compounds having concentration 100 µg/mL were prepared in dimethyl sulphoxide (DMSO). The solution of test compounds (1 mL) was transferred to test tubes having sterilized nutrient medium diluted serially to get a set of six dilutions of test compounds having concentrations 50, 25, 12.5, 6.25, 3.12 and 1.56 µg/mL. The 100 µL of freshly cultured strain in normal saline was transferred into each test tube for inoculation and incubated at 37 °C for 24 h for bacterial strains and 7 days at 25 °C for fungal strains. Ciprofloxacin and fluconazole were used as standard drugs for antibacterial and antifungal testing, respectively. Each sample was assayed in triplicate and the concordant MIC values were reported.

The molecular mechanics force field (MM) process of Hyperchem 6.03 (1993) was used for the pre-optimization of the structures of test compounds **1–20** and the resulting geometries were further refined by means of the semiempirical method PM3 (Parametric Method-3). A gradient norm limit of 0.01 kcal/A° was used for the geometry optimization. The lowest energy structure/configuration of each molecule was used for the calculation of molecular/structural parameters using TSAR 3.3 software for Windows (2000). The regression analysis was done using the SPSS software package (1999).

Synthesis of Schiff base ligands(1–4)

2-Hydroxy-1-naphthaldehyde (2 mmol), 2-amino-6-substituted benzothiazole derivatives (2 mmol) and 2–3 drops of glacial acetic acid were refluxed together in methanol (30 mL) for about 4–5 h. The solid obtained was dried, purified and recrystallised from ethanol. The purity of the compound was checked regularly with thin layer chromatography (TLC).

[1] (1-[(6-Ethoxy-benzothiazol-2-ylimino)-methyl]-naphthalen-2-ol)

Yield: 72%; yellow solid; m.p. 210–212 °C; (Mol. Wt. 348.09); Anal. Calcd for $C_{20}H_{16}N_2O_2S$ (%): C, 68.94; H, 4.63; N, 8.04. Found: C, 68.96; H, 4.64; N, 8.06. IR (KBr pellets, cm^{-1}): 3319 (s, ν_{O-H}), 1621 (s, $\nu_{C=N}$). ^{1}H NMR (DMSO-d_6, δ_H): 14.04 (1H, s, O–H), 10.03 (1H, s, HC=N), 8.55 (1H, d, $J = 8$ Hz, Ar–H), 8.15 (1H, s, Ar–H), 8.05 (1H, d, $J = 8$ Hz, Ar–H), 7.86 (1H, d, $J = 8$ Hz, Ar–H), 7.82 (1H, t, $J = 12$ Hz, Ar–H), 7.65 (1H, t, $J = 12$ Hz, Ar–H), 7.45 (1H, s, Ar–H), 7.22 (1H, d, $J = 8$ Hz, Ar–H), 7.09 (1H, d, $J = 8$ Hz, Ar–H), 4.12 (2H, q, OCH_2), 1.43 (3H, t, CH_3), ppm. ^{13}C NMR (DMSO-d_6, δ_C): 189.77 (C–OH), 178.72, 170.88, 159.89 (**C**=N), 146.41, 136.72, 135.13, 130.76, 129.53, 126.39, 124.50, 121.34, 119.70, 115.70, 108.46, 106.58 (s, Ar–C), 65.77 (s, C-OCH_2), 13.74 (s, C–CH_3).

[2] (1-[(6-Nitro-benzothiazol-2-ylimino)-methyl]-naphthalen-2-ol)

Yield: 72%; yellow solid; m.p. 202–204 °C; (Mol. Wt. 349.05); Anal. Calcd for $C_{20}H_{16}N_2O_2S$ (%): C, 61.88; H, 3.17; N, 12.03. Found: C, 61.56; H, 3.02; N, 11.83. IR (KBr pellets, cm^{-1}): 3310 (s, ν_{O-H}), 1615(s, $\nu_{C=N}$), 1550, 1350 (m, ν_{NO2}). ^{1}H NMR (DMSO-d_6, δ_H): 13.91 (1H, s, O–H), 9.90 (1H, s, HC = N), 8.43 (1H, d, $J = 8$ Hz, Ar–H), 8.02 (1H, s, Ar–H), 7.92 (1H, d, $J = 8$ Hz, Ar–H), 7.86 (1H, d, $J = 8$ Hz, Ar–H), 7.70 (1H, t, $J = 12$ Hz, Ar–H), 7.52 (1H, t, $J = 12$ Hz, Ar–H), 7.32 (1H, s, Ar–H), 7.11 (1H, d, $J = 8$ Hz, Ar–H), 6.96 (1H, d, $J = 8$ Hz, Ar–H) ppm. ^{13}C NMR (DMSO-d_6, δ_C): 188.63 (C–OH), 178.63, 170.91, 159.63 (**C**=N), 146.62, 136.24, 135.71, 130.85, 129.77, 126.76, 124.82, 121.65, 119.71, 115.14, 108.26, 106.70 (s, Ar–C).

[3] (1-[(6-Methoxy-benzothiazol-2-ylimino)-methyl]-naphthalen-2-ol)

Yield: 71%; yellow solid; m.p. 104–106 °C; (Mol. Wt. 334.08); Anal. Calcd for $C_{19}H_{14}N_2O_2S$ (%): C, 68.24; H, 4.22; N, 8.38. Found: C, 68.23; H, 4.21; N, 8.37. IR (KBr pellets, cm^{-1}): 3325 (s, ν_{O-H}), 1625 (s, $\nu_{C=N}$). ^{1}H NMR: (DMSO-d_6, δ_H): 13.99 (1H, s, O–H), 9.97 (1H, s, HC=N), 8.51 (1H, d, $J = 8$ Hz, Ar–H), 8.10 (1H, s, Ar–H), 8.00 (1H, d, $J = 8$ Hz, Ar–H), 7.80 (1H, d, $J = 8$ Hz, Ar–H), 7.76 (1H, t, $J = 12$ Hz, Ar–H), 7.40 (1H, t, $J = 12$ Hz), 7.18 (1H, s, Ar–H) 7.15 (1H, d, $J = 8$ Hz, Ar–H), 7.04 (1H, d, $J = 8$ Hz, Ar–H), 4.07 (3H, s, OCH_3). ^{13}C NMR (DMSO-d_6, δ_C): 186.86 (C–OH), 174.77, 163.61, 152.87 (**C**=N), 147.84, 140.28, 138.08, 135.54, 132.42, 129.30, 127.44, 123.33, 119.57, 115.21, 108.29, 106.71 (s, Ar–C), 64.68 (s, C–OCH_3).

[4] (1-[(6-Methyl-benzothiazol-2-ylimino)-methyl]-naphthalen-2-ol)

Yield: 71%; yellow solid; m.p. 112–114 °C; (Mol. Wt. 318.08); Anal. Calcd for $C_{19}H_{14}N_2OS$ (%): C, 71.67; H, 4.43; N, 8.80. Found: C, 71.65; H, 4.45; N, 8.77. IR (KBr pellets, cm^{-1}): 3405 (s, ν_{O-H}), 1621 (s, $\nu_{C=N}$). ^{1}H NMR: (DMSO-d_6, δ_H): 14.07 (1H, s, O–H), 10.06 (1H, s, C=N), 8.59 (1H, d, $J = 8$ Hz, Ar–H), 8.18 (1H, s, Ar–H), 8.08 (1H, d, $J = 8$ Hz, Ar–H), 7.91 (1H, d, $J = 8$ Hz, Ar–H), 7.86 (1H, t, $J = 12$ Hz, Ar–H), 7.69 (1H, t, $J = 12$ Hz, Ar–H), 7.49 (1H, s, Ar–H), 7.25 (1H, d, $J = 8$ Hz, Ar–H), 7.12 (1H, d, J = 8 Hz, Ar–H), 1.46 (3H, s, CH_3). ^{13}C NMR (DMSO-d_6, δ_C): 188.07 (s, C–OH), 175.98, 164.82, 154.08 (s, C=N), 149.05, 141.49, 139.29, 136.75, 133.63, 130.52, 128.65, 126.71, 124.54, 124.25, 120.49, 119.20, 115.15, 108.23, 106.33 (s, Ar–C), 12.21 (s, C–CH_3).

Synthesis of complexes (5–20)

The synthesized Schiff base ligands (HL) (1 mmol) and sodium metal (1 mmol) were refluxed in methanol (20 mL) for 2 h to get the sodium salt of Schiff base ligands to which (1 mmol) dialkyl/diaryltindichloride was added and refluxed for about 5–6 h. The reaction mixture was filtered and evaporated over rotary evaporator under reduced pressure. The collected solid was washed with a mixture of chloroform and dry hexane. A similar procedure was adopted for the synthesis of all other complexes.

[5] N-((2-(Chlorodiphenylstannyloxy)naphthalen-1-yl)methylene)-6-ethoxybenzo[d] thiazol-2-amine

Yield: 71%; brown solid; m.p. 217–220 °C; (Mol. Wt. 656.03); Anal. Calcd for $C_{32}H_{25}ClN_2O_2SSn$ (%): C, 58.61; H, 3.84; Cl, 5.41; N, 4.27; Sn, 18.10. Found: C, 58.58; H, 3.82; Cl, 5.43; N, 4.26; Sn, 18.12. IR (KBr pellets, cm^{-1}): 1601 (s, $\nu_{C=N}$), 604 (m, ν_{Sn-N}), 514 (m, ν_{Sn-C}), 405 (w, ν_{Sn-O}). ^{1}H NMR: (DMSO-d_6, δ_H): 10.85 (1H, s, HC=N), 8.55 (1H, d, $J = 8$ Hz, Ar–H), 8.09 (1H, s, Ar–H), 8.06 (1H, d, $J = 8$ Hz, Ar–H), 7.99 (1H, d, $J = 8$ Hz, Ar–H), 7.61 (1H, t, $J = 12$ Hz, Ar–H), 7.39 (1H, t, $J = 12$ Hz, Ar–H), 7.34–7.40 (10H, m, Ar–H), 7.32 (1H, s, Ar–H), 7.23 (1H, d, $J = 8$ Hz, Ar–H), 4.10 (2H, q, OCH_2), 1.44 (3H, t CH_3). ^{13}C NMR (DMSO-d_6, δ_C): 186.26 (C–OH), 176.86, 165.93, 156.50 (**C**=N), 143.34, 139.51, 138.99, 135.80, 133.92, 131.01, 132.65, 131.76, 128.91, 128.40, 127.99, 124.00, 123.86, 122.98, 120.38, 118.48, 115.10, 108.47, 106.29 (s, Ar–C), 65.18 (s, C–OCH_2), 16.18 (s, C–CH_3) ppm. ^{119} Sn NMR (DMSO-d_6, δ_{Sn}): −400.00 ppm.

[6] N-((2-(Dibutylchlorostannyloxy)naphthalen-1-yl)methylene)-6-ethoxybenzo[d] thiazol-2-amine

Yield: 68%; brown solid; m.p. 214–216 °C; (Mol. Wt. 616.10); Anal. Calcd for $C_{28}H_{33}ClN_2O_2SSn$ (%): C, 54.61; H, 5.40; Cl, 5.76; N, 4.55; Sn, 19.28. Found: C, 54.62; H, 5.42; Cl, 5.73; N, 4.57; Sn, 19.25. IR (KBr pellets, cm^{-1}): 1609 (s, $\nu_{C=N}$), 608 (m, ν_{Sn-N}), 512 (m, ν_{Sn-C}), 401 (w, ν_{Sn-O}). ^{1}H NMR: (DMSO-d_6, δ_H): 10.85 (1H, s, HC=N), 8.55 (1H, d, $J = 8$ Hz, Ar–H), 8.13 (1H, d, J = 8 Hz, Ar–H), 8.05 (1H, s, Ar–H), 7.87 (1H, d, $J = 8$ Hz, Ar–H), 7.83 (1H, d, $J = 8$ Hz, Ar–H), 7.65 (1H, t, $J = 12$ Hz, Ar–H), 7.45 (1H, t, $J = 12$ Hz, Ar–H), 7.23 (1H, s, Ar–H), 7.10 (1H, d, $J = 8$ Hz, Ar–H), 4.12 (2H, q, OCH_2), 4.11 (4H, m, Bu-H), 3.98 (4H, m, Bu-H), 1.43 (3H, s, CH_3), 1.37 (6H, t, Bu-H), 0.91 (4H, m, Bu-H) ppm. ^{13}C NMR (DMSO-d_6, δ_C): 189.77 (**C**–OH), 176.53, 165.37, 154.63 (**C**=N), 149.61, 142.04, 139.84, 137.30, 134.19, 131.07, 129.20, 127.26, 125.09, 124.80, 121.80, 121.04, 119.75, 115.70, 108.46, 106.58 (s, Ar–C), 64.56 (s, C-OCH_2), 30.98 (s, Bu–C), 20.96 (s, Bu–C), 14.03 (s, C–CH_3), 11.85 (s, Bu–C), 9.29 (s, Bu–C) ppm. ^{119}Sn NMR (DMSO-d_6, δ_{Sn}): −322.43 ppm.

[7] N-((2-(Chlorodiethylstannyloxy)naphthalen-1-yl)methylene)-6-ethoxybenzo[d] thiazol-2-amine

Yield: 69%; reddish brown; m.p. 217–219 °C; (Mol. Wt. 560.03); Anal. Calcd for $C_{24}H_{25}ClN_2O_2SSn$ (%): C, 51.50; H, 4.50; Cl, 6.33; N, 5.01; Sn, 21.21. Found: C, 51.53; H, 4.52; Cl, 6.35; N, 5.04; Sn, 21.24. IR (KBr pellets, cm^{-1}): 1605 (s, $\nu_{C=N}$), 615 (m, ν_{Sn-N}), 517 (m, ν_{Sn-C}), 405 (w, ν_{Sn-O}). ^{1}H NMR: (DMSO-d_6, δ_H): 10.76 (1H, s, HC=N), 8.58 (1H, d, $J = 8$ Hz, Ar–H), 8.13 (1H, s, Ar–H), 8.05 (1H, d, $J = 8$ Hz, Ar–H), 7.87 (1H, d, $J = 8$ Hz, Ar–H), 7.83 (1H, t, $J = 12$ Hz, Ar–H), 7.64 (1H, t, $J = 12$ Hz, Ar–H), 7.44 (1H, s, Ar–H), 7.23 (1H, d, $J = 8$ Hz, Ar–H), 7.10 (1H, d, $J = 8$ Hz, Ar–H), 4.13 (2H, q, OCH_2), 1.43 (4H, t, CH_3), 1.10 (4H, t, Et-H), 0.91 (6H, m, Et-H). ^{13}C NMR (DMSO-d_6, δ_C): 189.42 (s, C–OH), 177.22, 164.94, 155.83(s, C=N), 149.54, 141.54, 139.88, 137.01, 133.92, 131.66, 130.45, 129.78, 128.57, 126.99, 124.84, 119.48, 116.56, 108.45, 106.59 (s, Ar–C), 65.77 (s, C–OCH_2), 19.98 (s, C–CH_3), 14.03 (s, Et-C), 11.17 (s, Et-C) ppm. ^{119}Sn NMR (DMSO-d_6, δ_{Sn}): −287.14 ppm.

[8] N-((2-(Chlorodimethylstannyloxy)naphthalen-1-yl)methylene)-6-ethoxybenzo[d] thiazol-2-amine

Yield: 67%; reddish brown; m.p. 212–214 °C; (Mol. Wt. 532.00); Anal. Calcd for $C_{22}H_{21}ClN_2O_2SSn$ (%): C, 49.70; H, 3.98; Cl, 6.67; N, 5.27; O, Sn, 22.33. Found: C, 49.72; H, 3.95; Cl, 6.63; N, 5.24; Sn, 22.31. IR (KBr pellets, cm^{-1}): 1609 (s, $\nu_{C=N}$), 609 (ν_{Sn-N}), 512 (ν_{Sn-C}), 402 (ν_{Sn-O}), ^{1}H NMR: (DMSO-d_6, δ_H): 10.75, (1H, s, HC=N), 8.54 (1H, d, $J = 8$ Hz, Ar–H), 8.11 (1H, s, Ar–H), 8.03 (1H, d, $J = 8$ Hz, Ar–H), 7.86 (1H, d, $J = 8$ Hz, Ar–H), 7.82 (1H, t, $J = 12$ Hz, Ar–H), 7.63 (1H, t, $J = 12$ Hz, Ar–H), 7.43 (1H, t, $J = 12$ Hz, Ar–H), 7.22 (1H, d, J = 8 Hz, Ar–H), 7.09 (1H, d, $J = 8$ Hz, Ar–H), 4.12 (2H, q, OCH_2), 1.42 (3H, t, CH_3), 0.85 (6H, s, Me-H). ^{13}C NMR (DMSO-d_6, δ_C): 187.16 (s, C–OH), 175.07, 163.91, 153.17 (s, C=N), 148.14, 140.58, 138.83, 132.72, 129.60, 127.74, 125.80, 123.34, 119.58, 114.24, 108.88, 106.71, (s, Ar–C), 63.71 (s, C-OCH_2), 29.52 (s, Me-C), 10.11 (s, C–CH_3) ppm. ^{119}Sn NMR (DMSO-d_6, δ_{Sn}): −260.75 ppm.

[9] N-((2-(Chlorodiphenylstannyloxy)naphthalen-1-yl)methylene)-6-nitrobenzo[d] thiazol-2-amine

Yield: 72%, brown solid; m.p. 210–212 °C; (Mol. Wt. 656.99); Anal. Calcd for $C_{30}H_{20}ClN_3O_3SSn$ (%): C, 54.87; H, 3.07; Cl, 5.40; N, 6.40; Sn, 18.08. Found: C, 54.84; H, 3.05; Cl, 5.37; N, 6.43; Sn, 18.06. IR (KBr pellets, cm^{-1}): 1611 (s, $\nu_{C=N}$), 612 (m, ν_{Sn-N}), 505 (m, ν_{Sn-C}), 401 (w, ν_{Sn-O}),), ^{1}H NMR (DMSO-d_6, δ_H): 10.85 (1H, s, HC=N), 8.55 (1H, d, $J = 8$ Hz, Ar–H), 8.15 (1H, s, Ar–H), 8.06 (1H, d, $J = 8$ Hz, Ar–H), 7.91 (1H, d, $J = 8$ Hz, Ar–H), 7.85 (1H, t, $J = 12$ Hz, Ar–H), 7.61 (1H, t, $J = 12$ Hz, Ar–H), 7.58 (1H, s, Ar–H), 7.40–7.34 (10H, m, Ar–H), 7.31 (1H, d, $J = 8$ Hz, Ar–H) 7.27 (1H, d, $J = 8$ Hz, Ar–H), 7.22 (1H, d, J = 8 Hz, Ar–H). ^{13}C NMR (DMSO-d_6, δ_C): 185.11 (s, C–OH), 175.71, 164.77, 155.35 (s, C=N), 142.19, 138.35, 137.43, 134.63, 129.85, 127.76, 127.24, 126.44, 124.45, 122.84, 122.70, 121.83, 118.70, 114.79, 107.65, 105.60 (s, Ar–C) ppm. ^{119}Sn NMR (DMSO-d_6, δ_{Sn}): −359.85 ppm.

[10] N-((2-(Dibutylchlorostannyloxy)naphthalen-1-yl)methylene)-6-nitrobenzo[d] thiazol-2-amine

Yield: 62%; brown solid; m.p. 215–217 °C; (Mol. Wt. 617.06); Anal. Calcd for $C_{26}H_{28}ClN_3O_3SSn$ (%): C, 50.63; H, 4.58; Cl, 5.75; N, 6.81; Sn, 19.25. Found: C, 50.64; H, 4.57; Cl, 5.77; N, 6.83; Sn, 19.24. IR (KBr pellets, cm^{-1}): 1615 (s, $\nu_{C=N}$), 608 (m, ν_{Sn-N}), 511 (m, ν_{Sn-C}), 408 (w, ν_{Sn-O}). ^{1}H NMR: (DMSO-d_6, δ_H): 10.85 (1H, s, HC=N), 8.68 (1H, d, $J = 8$ Hz, Ar–H), 8.13 (1H, s, Ar–H), 8.05 (1H, d, $J = 8$ Hz, Ar–H), 7.87 (1H, d, $J = 8$ Hz, Ar–H), 7.83 (1H, d, $J = 8$ Hz, Ar–H), 7.65 (1H, t, $J = 12$ Hz, Ar–H), 7.45 (1H, t, $J = 12$ Hz, Ar–H), 7.23 (1H, s, Ar–H), 7.10 (1H, d, Ar–H), 4.00 (4H, m, Bu-H), 3.61 (4H, m, Bu-H), 1.43 (4H, m, Bu-H), 1.36 (6H, t, Bu-H). ^{13}C NMR (DMSO-d_6, δ_C): 188.36 (C–OH), 176.27, 165.12, 154.37 (**C**=N), 149.35, 141.79, 139.59, 137.04, 133.93, 130.81, 128.94, 127.00, 124.84, 124.54, 120.78, 119.49, 115.45,

108.71, 106.62 (s, Ar–C), 20.70, 13.77, 11.60, 9.04 (s, Bu–C) ppm. ^{119}Sn NMR (DMSO-d_6, δ_{Sn}): −320.49 ppm.

[11] N-((2-(Chlorodiethylstannyloxy)naphthalen-1-yl)methylene)-6-nitrobenzo[d] thiazol-2-amine

Yield: 70%; brown solid; m.p. 217–219 °C; (Mol. Wt. 560.99); Anal. Calcd for $C_{22}H_{20}ClN_3O_3SSn$ (%): C, 47.13; H, 3.60; Cl, 6.32; N, 7.50; Sn, 21.17. Found: C, 47.15; H, 3.62; Cl, 6.35; N, 7.53; Sn, 21.19. IR (KBr pellets, cm^{-1}): 1606 (s, $\nu_{C=N}$), 614 (ν_{Sn-N}), 505 (ν_{Sn-C}), 422 (ν_{Sn-O}). ^{1}H NMR: (DMSO-d_6, δ_H): 10.23 (1H, s, HC=N), 8.43 (1H, d, $J = 8$ Hz, Ar–H), 8.10 (1H, d, $J = 8$ Hz, Ar–H), 8.01 (1H, d, J = 8 Hz, Ar–H), 7.76 (1H, d, $J = 8$ Hz, Ar–H), 7.72 (1H, t, $J = 12$ Hz, Ar–H), 7.61 (1H, t, $J = 12$ Hz, Ar–H), 7.39 (1H, s, Ar–H), 7.21 (1H, d, $J = 8$ Hz, Ar–H), 7.02 (1H, d, $J = 8$ Hz, Ar–H), 1.13 (4H, q, Et-H), 0.96 (6H, t, Et-H). ^{13}C NMR (DMSO-d6, δ_C): 187.46 (C–OH), 175.37, 164.21, 153.47 (**C**=N), 148.44, 140.88, 138.68, 133.92, 131.66, 130.45, 129.78, 128.57, 126.99, 124.84, 119.48, 116.56, 108.45, 106.59 (s, Ar–C), 19.45, 11.60 (s, Et-C) ppm. ^{119}Sn NMR (DMSO-d_6, δ_{Sn}): −291.23 ppm.

[12] N-((2-(Chlorodimethylstannyloxy)naphthalen-1-yl)methylene)-6-nitrobenzo[d] thiazol-2-amine

Yield: 69%; brown solid; m.p. 197–199 °C; (Mol. Wt. 532.96); Anal. Calcd for $C_{20}H_{16}ClN_3O_3SSn$ (%): C, 45.10; H, 3.03; Cl, 6.66; N, 7.89; Sn, 22.29. Found: C, 45.13; H, 3.05; Cl, 6.64; N, 7.84; Sn, 22.27. IR (KBr pellets, cm^{-1}): 1601 (s, $\nu_{C=N}$), 610 (ν_{Sn-N}), 508 (ν_{Sn-C}), 424 (ν_{Sn-O}). ^{1}H NMR: (DMSO-d_6, δ_H): 10.77 (1H, s, HC=N), 8.63 (1H, d, $J = 8$ Hz, Ar–H), 8.15 (1H, s, Ar–H), 7.99 (1H, d, $J = 8$ Hz, Ar–H), 7.81 (1H, d, $J = 8$ Hz, Ar–H), 7.76 (1H, t, $J = 12$ Hz, Ar–H), 7.59 (1H, t, $J = 12$ Hz, Ar–H), 7.38 (1H, d, $J = 8$ Hz, Ar–H), 7.27 (1H, d, $J = 8$ Hz, Ar–H), 7.15 (1H, d, $J = 8$ Hz, Ar–H), 0.83 (6H, s, Me-H) ppm. ^{13}C NMR (DMSO-d_6, δ_C): 186.86 (C–OH), 174.77, 163.61, 152.87 (**C**=N), 147.84, 140.28, 138.08, 135.54, 132.42, 129.30, 127.44, 125.50, 123.33, 123.04, 119.28, 113.94, 108.58, 106.48 (s, Ar–C), 9.81 (s, Me-C) ppm. ^{119}Sn NMR (DMSO-d_6, δ_{Sn}): −225.24 ppm.

[13] N-((2-(Chlorodiphenylstannyloxy)naphthalen-1-yl)methylene)-6-methoxybenzo[d] thiazol-2-amine

Yield: 69%; brown solid; m.p. 202–204 °C; (Mol. Wt. 642.02); Anal. Calcd for $C_{31}H_{23}ClN_2O_2SSn$(%): C, 58.02; H, 3.61; Cl, 5.52; N, 4.37; Sn, 18.50. Found: C, 58.03; H, 3.63; Cl, 5.51; N, 4.35; Sn, 18.48. IR (KBr pellets, cm^{-1}): 1603 (s, $\nu_{C=N}$), 614 (m, ν_{Sn-N}), 503 (m, ν_{Sn-C}), 411 (w, ν_{Sn-O}). ^{1}H NMR: (DMSO-d_6, δ_H): 10.79 (1H, s, C=N), 8.48 (1H, d, $J = 8$ Hz, Ar–H), 8.10 (1H, s, Ar–H), 8.01 (1H, d, $J = 8$ Hz, Ar–H), 7.91 (1H, d, $J = 8$ Hz, Ar–H), 7.54 (1H, t, $J = 12$ Hz, Ar–H), 7.33 (1H, t, $J = 12$ Hz, Ar–H), 7.30–7.27 (10H, m, Ar–H), 7.25 (1H, s, Ar–H), 7.17 (1H, d, $J = 8$ Hz, Ar–H), 7.01 (1H, d, $J = 8$ Hz, Ar–H), 4.06 (3H, s, OCH_3) ppm. ^{13}C NMR (DMSO-d_6, δ_C): 186.68, 177.28, 166.34, 156.92 (**C**=N), 143.76, 139.92, 139.00, 136.21, 134.33, 131.42, 129.33, 128.81, 128.01, 124.41, 124.27, 123.40, 118.90, 115.51, 108.88, 106.71 (s, Ar–C), 65.60 (s, C–OCH_3) ppm. ^{119}Sn NMR (DMSO-d_6, δ_{Sn}): −375.09 ppm.

[14] N-((2-(Dibutylchlorostannyloxy)naphthalen-1-yl)methylene)-6-methoxybenzo[d] thiazol-2-amine

Yield: 71%, brownish red solid; m.p. 210–212 °C; (Mol. Wt. 602.08); Anal. Calcd for $C_{27}H_{31}ClN_2O_2SSn$ (%): C, 53.89; H, 5.19; Cl, 5.89; N, 4.66; Sn, 19.73. Found: C, 53.87; H, 5.21; Cl, 5.87; N, 4.64; Sn, 19.76. IR (KBr pellets, cm^{-1}): 1612 (s, $\nu_{C=N}$), 601 (m, $\nu_{Sn-N)}$, 508 (m, ν_{Sn-C}), 404 (w, ν_{Sn-O}), ^{1}H NMR: (DMSO-d_6, δ_H): 10.84 (1H, s, HC=N), 8.59 (1H, d, $J = 8$ Hz), 8.11 (1H, s, Ar–H), 8.05 (1H, d, $J = 8$ Hz, Ar–H), 7.86 (1H, d, $J = 8$ Hz, Ar–H), 7.82 (1H, t, $J = 12$ Hz, Ar–H), 7.64 (1H, t, $J = 12$ Hz, Ar–H), 7.44 (1H, s, Ar–H), 7.22 (1H, d, $J = 8$ Hz, Ar–H), 7.09 (1H, d, $J = 8$ Hz, Ar–H), 4.13 (3H, s, OCH_3), 3.99 (4H, m, Bu-H), 3.58 (4H, m, Bu-H), 1.42 (4H, m, Bu-H), 1.35 (6H, t, Bu-H) ppm. ^{13}C NMR (DMSO-d_6, δ_C): 188.73 (C–OH), 176.65, 165.49, 154.75 (**C**=N), 149.72, 142.16, 139.96, 137.41, 134.30, 131.18, 129.31, 127.38, 125.21, 124.91, 121.16, 119.86, 115.82, 108.26, 106.99 (s, Ar–C), 64.68 (s, OCH_3), 21.08, 14.14, 11.97, 9.41 (s, Bu–C) ppm. ^{119}Sn NMR (DMSO-d_6, δ_{Sn}): −302.18 ppm.

[15] N-((2-(Chlorodiethylstannyloxy)naphthalen-1-yl)methylene)-6-methoxybenzo[d] thiazol-2-amine

Yield: 68%; brown solid; m.p. 204–206 °C; (Mol. Wt. 546.02); Anal. Calcd for $C_{23}H_{23}ClN_2O_2SSn$ (%): C, 50.63; H, 4.25; Cl, 6.50; N, 5.13; Sn, 21.75. Found: C, 50.65; H, 4.27; Cl, 6.53; N, 5.15; Sn, 21.78. IR (KBr pellets, cm^{-1}): 1609 (s, $\nu_{C=N}$), 615 (m, ν_{Sn-N}), 513 (m, ν_{Sn-C}), 407 (w, ν_{Sn-O}). ^{1}H NMR: (DMSO-d_6, δ_H): 10.79 (1H, s, HC=N), 8.61 (1H, d, $J = 8$ Hz, Ar–H), 8.19 (1H, s, Ar–H), 8.09 (1H, d, $J = 8$ Hz, Ar–H), 7.92 (1H, d, $J = 8$ Hz, Ar–H), 7.85 (1H, t, $J = 12$ Hz, Ar–H), 7.69 (1H, t, $J = 12$ Hz, Ar–H), 7.49 (1H, s, Ar–H), 7.25 (1H, d, $J = 8$ Hz, Ar–H), 7.14 (1H, d, $J = 8$ Hz, Ar–H), 4.07 (3H, s, OCH_3), 1.16 (4H, q, Et-H), 0.93 (6H, t, Et-H) ppm. ^{13}C NMR (DMSO-d_6, δ_C): 186.17, 174.08, 162.93, 152.18 (**C**=N), 147.16, 139.60, 137.40, 134.85, 131.74, 128.62, 126.75, 124.81, 122.65, 122.35, 118.59, 115.31, 106.97 (s, Ar–C), 62.11 (s, C–OCH_3) 28.53, 9.12 (s, Et-C). ^{119}Sn NMR (DMSO-d_6, δ_{Sn}): −279.12 ppm.

[16] N-((2-(Chlorodimethylstannyloxy)naphthalen-1-yl)methylene)-6-methoxybenzo[d] thiazol-2-amine

Yield: 67%; brown solid; m.p. 208–210 °C; (Mol. Wt. 517.99); Anal. Calcd for $C_{21}H_{19}ClN_2O_2SSn$ (%): C, 48.73; H, 3.70; Cl, 6.85; N, 5.41; Sn, 22.93. Found: C, 48.72; H, 3.74; Cl, 6.83; N, 5.43; Sn, 22.95. IR (KBr pellets, cm^{-1}): 1605 (s, $\nu_{C=N}$), 602 (m, ν_{Sn-N}), 507 (m, ν_{Sn-C}), 402 (w, ν_{Sn-O}). ^{1}H NMR: (DMSO-d_6, δ_H): 10.75 (1H, s, HC=N), 8.58 (1H, d, $J = 8$ Hz, Ar–H), 8.11 (1H, s, Ar–H), 8.05 (1H, d, $J = 8$ Hz, Ar–H), 7.86 (1H, d, $J = 8$ Hz, Ar–H), 7.84 (1H, t, $J = 12$ Hz, Ar–H), 7.63 (1H, t, $J = 12$ Hz), 7.43 (1H, s, Ar–H), 7.22 (1H, d, Ar–H), 7.09 (1H, d, Ar–H), 4.11 (3H, s, OCH_3), 0.87 (6H, s, Me-H) ppm. ^{13}C NMR (DMSO-d_6, δ_C): 185.99 (C–OH), 173.50, 162.34, 151.60 (**C**=N), 146.57, 139.01, 136.81, 134.26, 131.15, 128.03, 126.17, 124.23, 122.06, 121.77, 118.01, 112.67, 107.31, 105.14 (s, Ar–C), 61.53 (s, C–OCH_3), 8.54 (s, Me-C) ppm. ^{119}Sn NMR (DMSO-d_6, δ_{Sn}): −256.67 ppm.

[17] N-((2-(Chlorodiphenylstannyloxy)naphthalen-1-yl)methylene)-6-methylbenzo[d] thiazol-2-amine

Yield: 73%; brown solid; m.p. 214–216 °C; (Mol. Wt. 626.02); Anal. Calcd for $C_{31}H_{23}ClN_2OSSn$ (%): C, 59.50; H, 3.70; Cl, 5.67; N, 4.48; Sn, 18.97. Found: C, 59.51; H, 3.72; Cl, 5.63; N, 4.46; Sn, 18.95. IR (KBr pellets, cm^{-1}): 1608 (s, $\nu_{C=N}$), 606 (m, ν_{Sn-N}), 517 (m, ν_{Sn-C}), 425 (w, ν_{Sn-O}). ^{1}H NMR: (DMSO-d_6, δ_H): 10.82 (1H, s, HC=N), 8.51 (1H, d, $J = 8$ Hz, Ar–H), 8.12 (1H, s, $J =$ Ar–H), 8.03 (1H, d, $J = 8$ Hz, Ar–H), 7.90 (1H, d, $J = 8$ Hz, Ar–H), 7.81 (1H, t, $J = 12$ Hz, Ar–H), 7.59 (1H, t, $J = 12$ Hz, Ar–H), 7.36 (1H, s, Ar–H), 7.28–7.33 (10H, m, Ar–H), 7.23 (1H, d, $J = 8$ Hz, Ar–H), 7.18 (1H, d, $J = 8$ Hz, Ar–H), 1.34 (3H, s, CH_3) ppm. ^{13}C NMR (DMSO-d_6, δ_C) 184.79 (C–OH), 175.39, 164.46, 155.03 (**C**=N), 141.87, 138.04, 137.12, 134.33, 129.54, 127.44, 126.93, 126.12, 124.13, 122.53, 122.39, 121.51, 118.38, 114.48, 107.33, 105.29 (s, Ar–C), 14.76 (s, C–CH_3). ^{119}Sn NMR (DMSO-d_6, δ_{Sn}): −366.34 ppm.

[18] N-((2-(Dibutylchlorostannyloxy)naphthalen-1-yl)methylene)-6-methylbenzo[d] thiazol-2-amine

Yield: 69%; brown solid; m.p. 178-180 °C; (Mol. Wt. 586.09); Anal. Calcd for $C_{27}H_{31}ClN_2OSSn$ (%): C, 55.36; H, 5.33; Cl, 6.05; N, 4.78; Sn, 20.27. Found: C, 55.37; H, 5.35; Cl, 6.04; N, 4.76; Sn, 20.25. IR (KBr pellets, cm^{-1}): 1605 (s, $\nu_{C=N}$), 609 (m, ν_{Sn-N}), 518 (m, ν_{Sn-C}), 414 (w, ν_{Sn-O}), ^{1}H NMR: (DMSO-d_6, δ_H): 10.89 (1H, s, HC=N), 8.61 (1H, d, $J = 8$ Hz, Ar–H), 8.16 (1H, s, Ar–H), 8.07 (1H, d, J = 8 Hz, Ar–H), 7.91 (1H, d, $J = 8$ Hz, Ar–H), 7.87 (1H, t, $J = 12$ Hz, Ar–H), 7.69 (1H, t, $J = 12$ Hz, Ar–H), 7.49 (1H, s, Ar–H), 7.27 (1H, d, $J = 8$ Hz, Ar–H), 7.14 (1H, d, Ar–H), 4.04 (4H, m, Bu-H), 3.65 (4H, m, Bu-H), 1.48 (4H, m, Bu-H), 1.42 (6H, t, Bu-H), 1.29 (3H, s, CH_3). ^{13}C NMR (DMSO-d_6, δ_C): 188.07, 175.98, 164.82, 154.08 (**C**=N), 149.05, 141.49, 139.29, 136.75, 133.63, 130.52, 128.65, 126.71, 124.54, 124.25, 120.49, 119.20, 115.15, 108.42, 106.33 (s, Ar–C), 20.21 (s, Bu–C), 13.48 (s, C–CH_3), 11.30, 9.41, 8.74 (s, Bu-H) ppm. ^{119}Sn NMR (DMSO-d_6, δ_{Sn}): −322.24 ppm.

[19] N-((2-(Chlorodiethylstannyloxy)naphthalen-1-yl)methylene)-6-methylbenzo[d] thiazol-2-amine

Yield: 69%, reddish brown solid; m.p. 183–185 °C; (Mol. Wt. 530.02); Anal. Calcd for $C_{23}H_{23}ClN_2OSSn$ (%): C, 52.15; H, 4.38; Cl, 6.69; N, 5.29; Sn, 22.41. Found: C, 52.17; H, 4.41; Cl, 6.71; N, 5.31; Sn, 22.45. IR (KBr pellets, cm^{-1}): 1610 (s, $\nu_{C=N}$), 615 (m, ν_{Sn-N}), 513 (m, ν_{Sn-C}), 413 (w, ν_{Sn-O}). ^{1}H NMR (DMSO-d_6, δ_H): 10.89 (1H, s, HC=N), 8.56 (1H, d, $J = 8$ Hz, Ar–H), 8.19 (1H, s, Ar–H), 7.93 (1H, d, $J = 8$ Hz, Ar–H), 7.86 (1H, d, $J = 8$ Hz, Ar–H), 7.68 (1H, t, $J = 12$ Hz, Ar–H), 7.47 (1H, t, $J = 12$ Hz, Ar–H), 7.26 (1H, s, Ar–H), 7.15 (1H, d, $J = 8$ Hz, Ar–H), 7.01 (1H, d, $J = 8$ Hz, Ar–H), 1.42 (3H, s, CH_3), 1.13 (4H, q, Et-H), 0.92 (6H, t, Et-H) ppm. ^{13}C NMR (DMSO-d_6, δ_C): 185.59 (C–OH), 173.50, 162.34, 151.60 (C=N), 146.57, 139.01, 136.81, 134.26, 131.15, 128.03, 126.17, 124.23, 122.06, 121.77, 118.01, 114.73, 107.45, 106.39 (Ar–C), 27.95 (s, C–CH_3), 17.26, 8.54 (s, Et-C) ppm. ^{119}Sn NMR (DMSO-d_6, δ_{Sn}): −280.67 ppm.

[20] N-((2-(Chlorodimethylstannyloxy)naphthalen-1-yl)methylene)-6-methylbenzo[d] thiazol-2-amine

Yield: 66%, reddish brown solid; m.p. 191–193 °C; (Mol. Wt. 501.99); Anal. Calcd for $C_{21}H_{19}ClN_2OSSn$ (%): C, 50.28; H, 3.82; Cl, 7.07; N, 5.58; Sn, 23.67. Found: C, 50.30; H, 3.85; Cl, 7.06; N, 5.59; Sn, 23.65. IR (KBr pellets, cm^{-1}): 1605 (s, $\nu_{C=N}$), 610 (m, ν_{Sn-N}), 509 (m, ν_{Sn-C}), 410 (w, ν_{Sn-O}). ^{1}H NMR (DMSO-d_6, δ_H): 10.75 (1H, s, HC=N), 8.53 (1H, d, $J = 8$ Hz, Ar–H), 8.11 (1H, s, Ar–H), 8.05 (1H, d, $J = 8$ Hz, Ar–H), 8.02 (1H, d, $J = 8$ Hz, Ar–H), 7.86 (1H, t, $J = 12$ Hz, Ar–H), 7.65 (1H, t, $J = 12$ Hz, Ar–H), 7.43 (1H, s, Ar–H), 7.22 (1H, d, $J = 8$ Hz, Ar–H), 7.09 (1H, d, $J = 8$ Hz, Ar–H), 1.38 (3H, s, CH_3), 0.87 (6H, s, Me-H) ppm. ^{13}C NMR (DMSO-d_6, δ_C): 186.50, 174.41, 163.25, 152.15 (**C**=N), 147.48, 139.92, 137.72, 135.17, 132.06, 128.94, 127.08, 125.14, 122.97, 122.68, 118.92, 113.58, 108.22, 106.05 (s, Ar–H), 20.07 (s, C–CH_3), 9.45 (s, Me-C) ppm. ^{119}Sn NMR (DMSO-d_6, δ_{Sn}): −266.72 ppm.

Results and discussion

Synthetic aspects

The reaction of 2-hydroxy-1-naphthaldehyde with 2-amino-6-substituted benzothiazole (where $R = -OC_2H_5$, $-NO_2$, $-OCH_3$, $-CH_3$) led to the formation of (1-[(6-substituted-benzothiazol-2-ylimino)-methyl]-naphthalen-2-ol). The sodium salt of the ligand was prepared using sodium metal which was then treated with R_2SnCl_2, yielding the complexes (**5–20**) as shown in Scheme 1. These were isolated as air-stable coloured powders, with solubility in DMSO and low solubility in chloroform. The purity was checked by thin layer chromatography (TLC). The molar conductance of the complexes with 10^{-3} M solutions has very low value (8.0–17.0 $O^{-1}cm^2$ mol^{-1}) which clearly indicates the nonelectrolytic nature of the complexes.

IR spectra

The IR spectra of the prepared compounds were assigned after comparing with the ligands and the corresponding organotin(IV) complexes. The explicit feature seen in the IR spectra of complexes was the disappearance of broad absorption band of OH from the range 3405–3310 cm^{-1} which was due to the deprotonation of phenolic group from subsequent ligands (Mohammadi and Zahedi 2012). The strong-to-medium absorption bands in the IR spectra for the azomethine group of ligands were observed the range 1625–1615 cm^{-1} with a shift of 10–24 cm^{-1} towards lower frequencies with medium absorption bands on the formation of complexes. The Sn–O, Sn–C and Sn–N vibrations were found in the ranges 615–601, 518–503 and 425–401 cm^{-1}, respectively, showed coordination of nitrogen of azomethine, carbon of alkyl group and oxygen of phenolic group to the central tin atom (Nidhi and Malhotra 2011, Asija et al. 2012, Singh et al. 2010).

NMR spectroscopy

^{1}H NMR

The ^{1}H, ^{13}C, ^{119}Sn NMR spectra of the ligands and the complexes were recorded in DMSO. The ^{1}H NMR spectra of the compounds are based on integration values, coupling constants and chemical shifts. The monobasic bidentate Schiff base ligands revealed phenolic proton (OH) signal at δ 14.07–13.91 ppm. All the organotin(IV) complexes showed the absence of such a signal suggesting the deprotonation of the phenolic OH of the Schiff base and coordination to the tin atom on the formation of complexes. The characteristic chemical shifts in the ^{1}H NMR spectra of compounds with a signal at δ 10.06–9.90 ppm revealed the presence of azomethine

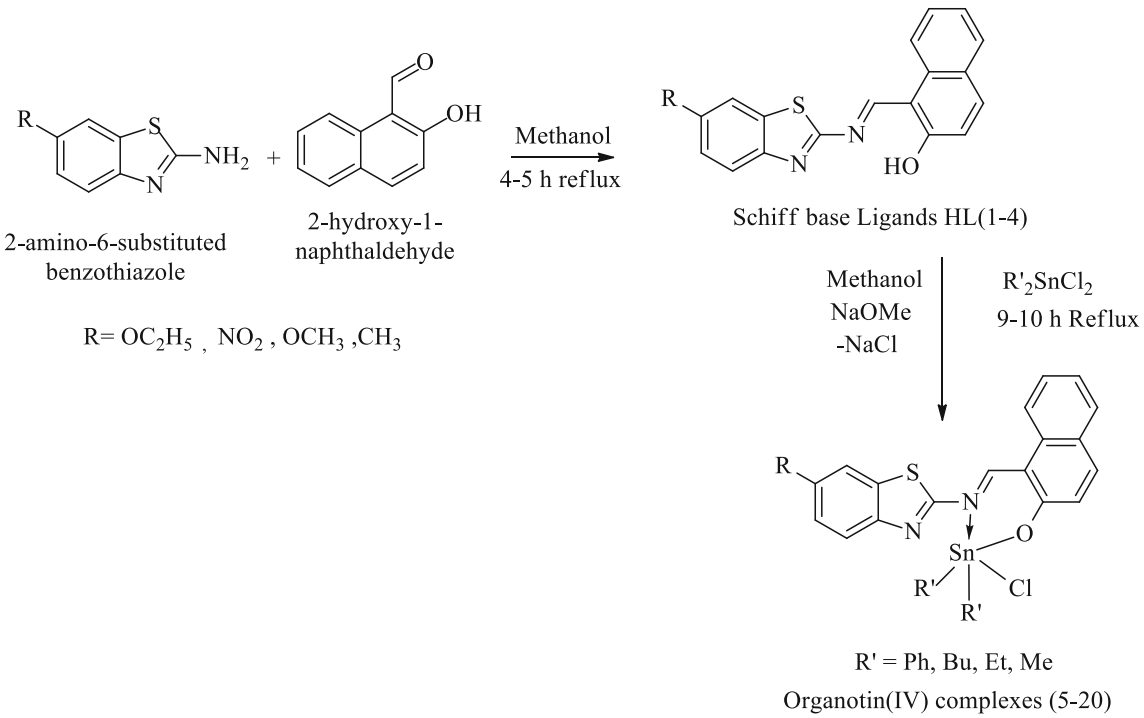

Scheme 1 Scheme for the synthesis of Schiff base ligands and organotin(IV) complexes

proton confirming the condensation of benzothiazole derivatives with 2-hydroxy-1-naphthaldehyde and the proton signals of azomethine group were shifted by δ 0.2–0.8 ppm which may be due to the coordination of nitrogen atom of azomethine group to the tin atom leading to significant deshielding effect (Gonzalez et al. 2009). The signals at δ 8.59–6.96 ppm were assigned to aryl protons of the ligands and the complexes. The ^{1}H NMR spectra of the dimethyltin complexes show the signal of Sn–CH_3 at 0.91–0.83 ppm. The coupling constant ^{2}J(Sn–CH_3) for the dimethyltin complexes was observed at about 76 Hz, as a consequence the major structural features of the solid state is retained in solution which supported the pentacoordinated environment around the tin atom (Yin and Chen 2006, Yin et al. 2005).

^{13}C NMR

The ^{13}C NMR spectra of the ligands showed the signal for C–OH at δ 189.77–188.56 ppm which get shifted due to coordination of oxygen to the central tin atom indicating formation of complexes. The carbons attached to thiazole group appeared in the range δ 178.72–163.61 ppm which shifted because of deshielding effect due to the presence of nearby azomethine nitrogen. The azomethine carbon appeared in the range δ 159.89–152.87 ppm which shifted downfield on complexation indicating involvement of nitrogen in coordination bonding to form complexes (Nidhi and Malhotra 2011, Asija et al. 2012). The aromatic carbons appeared in the aromatic range δ 149.05–105.29 ppm in ligands and complexes with slight alteration. The aliphatic carbons appeared in the aliphatic range δ 63.77–8.74 ppm in ligands and complexes.

^{119}Sn NMR

A sharp singlet was appeared in the ^{119}Sn spectra of the compounds in the range δ −400.00 to −359.85 ppm, δ −322.43 to −302.18 ppm, δ −291.23 to −279.12 ppm and δ 266.72 to −225.24 ppm for phenyl, butyl, ethyl and methyl complexes, respectively. These chemical shifts revealed the formation of pentacoordinated tin centres in the complexes in which the most electronegative atoms occupy the axial position and the nitrogen atom occupied the equatorial position (Devi et al. 2012). The chemical shift of ^{119}Sn spectra was affected by the nature of alkyl group which is attached to the tin atom directly. The phenyltin complexes showed high-field chemical shifts as an outcome of anisotropic shielding effects as well as the pi interactions (Sedaghat and Shokohi-pour 2009).

X-ray powder diffraction analysis

X-ray diffraction analyses of compounds exhibit the crystalline peak in the complexes. Powder XRD of all the other compounds exhibited their crystalline nature. The average crystallite size d_{XRD} of the compounds was calculated by Debye–Scherrer formula and was found approximately 26 nm. The XRD pattern of organotin(IV) complex **5** is presented in Fig. 1 (in supplementary data).

$$d_{XRD} = \frac{0.94\lambda}{\beta \frac{1}{2}\cos\theta}$$

where λ is wavelength, θ is diffraction angle, and β is full width at half maxima. The XRD powder diffraction analysis of the compounds revealed that the compounds were crystalline in nature.

In vitro antimicrobial activity

The in vitro biological activities (antibacterial and antifungal activities) of all the Schiff base ligands and their organotin(IV) complexes were evaluated against Gram-positive bacteria *B. cereus*, *S. aureus*, Gram-negative bacteria *E. coli*, *P. aeruginosa* and fungi *A. niger* and *A. flavus*. Ciprofloxacin and fluconazole were used as standard drugs for antibacterial and antifungal activities, respectively. The serial dilution method was used for the evaluation of antimicrobial activity. The results of antimicrobial activity in terms of MIC (minimum inhibitory concentration μM/mL) are presented in Table 1.

The results of antibacterial activity testing against *E. coli* indicated that compounds **5**, **9** and **17** were highly active with pMIC values of 2.021, 2.022 and 2.001 μM/mL, respectively. These compounds (**5**, **9** and **17**) have got ethoxy, nitro and methyl groups as substituent on phenyl ring of benzothiazole, respectively. In addition, two phenyl groups were attached to the tin metal in the structure of these compounds. The compounds **1** and **20** were found to be least active with pMIC values of 1.45 and 1.603 μM/mL, respectively.

In case of antimicrobial activity of synthesized compounds against *B. cereus*, *S. aureus*, *P. aeruginosa, A. niger* and *A. flavus*, compounds **5**, **9** and **13** had emerged as the most active ones and these compounds have ethoxy, nitro and methoxy groups, respectively, as substituents on phenyl ring of the benzothiazole ring in their structure. Compounds **3** and **4** were least active against *B. cereus*, *S. aureus*, *A. flavus* and *P. aeruginosa* and compounds **4** and **14** were least active against *A. niger*.

In general, it was observed that the metal complexes were more active than their respective Schiff bases and overall compounds **5** and **9** were found to be active against all the tested microbial strains and their activity was almost

Table 1 Antimicrobial activity of synthesized compounds (μM/mL)

Comp.	$pMIC_{ec}$	$pMIC_{pa}$	$pMIC_{bc}$	$pMIC_{sa}$	$pMIC_{an}$	$pMIC_{af}$
1	1.445	1.746	1.445	1.746	2.048	1.746
2	1.747	1.747	1.446	1.747	2.049	1.747
3	1.728	1.728	1.427	1.728	2.030	1.728
4	1.707	1.707	1.406	1.707	2.009	1.707
5	2.021	2.323	2.323	2.624	2.624	2.323
6	1.994	2.295	2.295	2.278	2.596	2.295
7	1.651	2.254	1.952	1.952	2.254	2.254
8	1.930	2.231	1.930	1.930	2.231	2.231
9	2.022	2.323	2.323	2.624	2.624	2.323
10	1.693	2.296	2.296	2.597	2.597	2.296
11	1.953	2.255	1.953	2.237	2.255	2.255
12	1.931	2.232	1.931	2.215	2.232	2.232
13	1.710	2.313	2.313	2.614	2.614	2.313
14	1.984	2.285	2.285	2.268	1.984	2.285
15	1.941	1.941	1.941	1.941	2.544	2.243
16	1.617	1.918	1.918	1.918	2.521	2.220
17	2.001	2.302	2.302	2.603	2.603	2.302
18	1.972	2.274	2.274	2.256	2.575	2.274
19	1.627	2.230	1.928	1.928	2.230	2.230
20	1.603	2.206	1.904	1.904	2.206	2.206
Std.	2.61*	2.61*	2.61*	2.61*	2.64#	2.64#

* Ciprofloxacin (antibacterial drug); # fluconazole (antifungal drug)

equivalent to the activity of standard drugs in case of *S. aureus* and *A. niger*. From the observed results, it was seen that there was a remarkable boost in the activity of complexes than the ligands. The increase in the antimicrobial activity of synthesized complexes can be attributed to the outcome of the chelation theory which coveys that due to chelation, complexes become very influencing, effective, intoxicating as chelation tends to formulate ligands to operate as more influential and better antimicrobial agents, hence tackling the microorganisms in a better way than the ligand. In addition, the π-electron delocalization partially shared with the donor atom of the coordinated ligand over the metal positive charge may increase the lipophilic character of the synthesized compounds due to which they permeate through lipid microbial membrane and the activity pattern followed was $NO_2 > OCH_3 > OC_2H_5$ because the capability of electron-withdrawing group increases the antimicrobial activity (Sharma et al. 2004, Judge et al. 2012a, b). The bond strength, solubility, conductivity between metal and ligand may also be the reason for enhancement in the activity. The hydrogen bond formation between oxygen atom and the azomethine nitrogen with the active centres of the cell constituent may influence the mode of action with the cell processes. The impermeability and the difference in the number of the ribosomes of cells of the microorganisms may also be responsible for the efficacy of the compounds (Kashar 2014, Sallam and Orabi 2002, Sharma et al. 2015).

QSAR analysis

Quantitative structure–activity relationship (QSAR) analysis for the in vitro antimicrobial activity and structural descriptors coding for various molecular properties of the twenty compounds (four ligands and sixteen organotin(IV) complexes of Schiff bases derived from 2-amino-6-substituted benzothiazole derivatives and 2-hydroxy-1-naphthaldehyde) were carried out to find out the mathematical relationship between alteration in structure and antimicrobial activity using the linear free energy relationship model (LFER) described by Hansch and Fujita (1964). The dependent variable pMIC (i.e. −log MIC) used as in QSAR study was obtained by taking negative logarithm of observed antimicrobial activities (i.e. MIC). The structural descriptors like log of octanol–water partition coefficient (log P), molar refractivity (MR), Kier's zero-, first-, second- and third-order molecular connectivity ($^0\chi$, $^0\chi^v$, $^1\chi$, $^1\chi^v$, $^2\chi$, $^2\chi^v$, $^3\chi$, $^3\chi^v$) and kappa shape (κ_1, κ_2, κ_3, $\kappa\alpha_1$, $\kappa\alpha_2$, $\kappa\alpha_3$) topological indices, Randic topological index (R), Wiener topological index (W), Balaban topological index (J), total energy (Te), energies of highest occupied molecular orbital (HOMO) and lowest unoccupied molecular orbital (LUMO), dipole moment (μ), nuclear repulsion energy (Nu.E) and electronic energy (Ele.E), calculated for organotin(IV) complexes of Schiff bases derived from 2-amino-6-substituted benzothiazole derivatives and 2-hydroxy-1-naphthaldehyde are presented in Table 2 (Hansch et al. 1973, Kier and Hall 1976, Randic et al. 1975, Balaban 1982, Wiener 1947, Randic 1993).

The antimicrobial activities and molecular descriptors for 20 compounds (Schiff base ligands **1–4** and their corresponding organotin(IV) complexes **5–20**) were subjected to linear free energy regression analysis for QSAR model development. The correlation between molecular descriptors and antimicrobial activities was analysed on the basis of regression analysis and correlation matrix constructed for antifungal activity against *Aspergillus flavus* is presented in Table 3 (in supplementary materials). The statistical relationships of different molecular descriptors with antimicrobial activities are presented in Table 4 (in supplementary materials). On the whole, high colinearity ($r > 0.8$) was observed between different parameters, i.e. molecular descriptors. The high interrelationship was observed between first-order kappa shape index, κ_1 and electronic energy, Ele.E ($r = 0.998$), Ele.E and zero-order molecular connectivity index, $^0\chi$ ($r = 0.998$), $^0\chi$ and κ_1 ($r = 0.994$) and low interrelationship was observed between second-order kappa shape index, κ_2 and Balaban index, J ($r = 0.000$) and κ_1 and J ($r = 0.032$). The correlation matrix indicated that the antimicrobial activity of

Table 2 Values of selected molecular descriptors for the synthesized compounds used in the QSAR analysis

Comp.	$^{0}\chi$	$^{0}\chi^{v}$	$^{1}\chi$	$^{1}\chi^{v}$	$^{2}\chi$	$^{2}\chi^{v}$	$^{3}\chi$	κ_1	κ_2	*R*	*J*	Te	Ele.E	LUMO	HOMO	*M*
1	17.225	14.522	12.242	8.908	10.830	6.628	1.416	18.367	8.347	12.242	1.126	−4028.010	−27551.000	−1.126	−8.494	2.488
2	17.389	13.670	12.114	8.297	11.179	6.474	1.712	18.367	7.935	12.114	1.137	−4226.910	−27467.800	−1.960	−9.006	7.425
3	16.518	13.814	11.742	8.321	10.449	6.399	1.416	17.416	7.709	11.742	1.137	−3872.230	−25844.600	−1.142	−8.517	2.564
4	15.811	13.406	11.204	8.208	10.280	6.536	1.501	16.468	7.087	11.204	1.146	−3552.250	−23867.400	−1.163	−8.594	1.236
5	26.658	25.842	19.136	21.539	16.992	21.310	2.329	29.089	13.533	19.136	1.051	−6144.810	−55530.400	−1.700	−8.336	3.983
6	24.675	25.312	17.047	22.537	14.834	23.438	2.274	28.019	13.693	17.047	1.282	−5745.980	−51206.500	−1.288	−8.305	2.457
7	21.847	22.483	15.047	20.537	13.334	23.135	2.274	24.135	10.951	15.047	1.246	−5122.700	−41673.800	−1.284	−8.299	2.171
8	20.433	21.069	13.926	21.109	13.377	23.220	2.908	22.203	9.647	13.926	1.215	−4811.090	−36780.600	−1.444	−8.409	5.995
9	26.821	24.991	19.009	20.928	17.342	21.156	2.624	29.089	13.107	19.009	1.056	−6344.300	−55862.900	−1.929	−8.709	9.522
10	24.838	24.460	16.920	21.925	15.184	23.284	2.570	28.019	13.181	16.920	1.289	−5945.180	−51023.400	−1.747	−8.668	8.896
11	22.010	21.632	14.920	19.925	13.684	22.982	2.570	24.135	10.508	14.920	1.255	−5321.880	−41582.300	−1.745	−8.667	8.901
12	20.596	20.217	13.799	20.498	13.727	23.067	3.204	22.203	9.240	13.799	1.225	−5010.270	−36789.600	−1.757	−8.701	8.775
13	25.951	25.135	18.636	20.951	16.612	21.081	2.329	28.135	12.887	18.636	1.060	−5989.280	−53856.600	−1.621	−8.315	2.773
14	23.968	24.605	16.547	21.949	14.454	23.209	2.274	27.046	12.992	16.547	1.291	−5590.200	−49069.200	−1.294	−8.321	2.498
15	21.140	21.776	14.547	19.949	12.954	22.906	2.274	23.168	10.292	14.547	1.258	−4966.900	−39749.400	−1.292	−8.314	2.585
16	19.725	20.362	13.426	20.521	12.997	22.991	2.908	21.240	9.013	13.426	1.227	−4655.310	−34887.800	−1.457	−8.423	5.804
17	25.244	24.727	18.098	20.839	16.443	21.218	2.413	27.184	12.250	18.098	1.068	−5669.050	−50766.400	−1.725	−8.378	4.117
18	23.261	24.196	16.009	21.837	14.285	23.346	2.358	26.074	12.301	16.009	1.297	−5270.290	−46444.400	−1.471	−8.329	1.364
19	20.433	21.368	14.009	19.837	12.785	23.044	2.358	22.203	9.647	14.009	1.265	−4646.940	−37395.900	−1.307	−8.341	2.629
20	19.018	19.954	12.888	20.409	12.828	23.129	2.992	20.280	8.394	12.888	1.235	−4335.330	−32698.600	−1.478	−8.456	4.919

synthesized complexes is controlled mainly by topological parameter, i.e. molecular connectivity indices.

The antifungal activity of synthesized derivatives against *A. flavus* is governed by the valence first-order molecular connectivity index, $^{1}\chi^{v}$ (Eq. 1).

QSAR model for antifungal activity against *A. flavus*

$$\begin{aligned} &p\mathrm{MIC}_{\mathrm{an}} = 0.042\,{}^{1}\chi^{v} + 1.377 \\ &n = 20 \quad r = 0.991 \quad r^2 = 0.981 \quad q^2 = 0.978 \\ &s = 0.031 \quad \mathrm{F} = 939.521 \end{aligned} \tag{1}$$

Here and thereafter, n is the number of data points, r correlation coefficient, r^2 squared correlation coefficient, q^2 cross-validated r^2 obtained by leave one out method, s standard error of the estimate and F Fischer statistics.

The QSAR model represented by Eq. (1) for antifungal activity against *A. flavus* depicted the importance of valence first-order molecular connectivity index, $^{1}\chi^{v}$ in controlling the antifungal activity of the synthesized derivatives. The topological indices are numerical quantifiers of molecular topology and are sensitive to bonding pattern, symmetry, content of heteroatom as well as degree of complexity of atomic neighbourhoods. The valence first-order molecular connectivity topological index ($^{1}\chi^{v}$) represents the molecules with branched structure (Lather and Madan 2005). The regression model represented by Eq. (1) demonstrated the positive correlation between valence first-order molecular connectivity index, $^{1}\chi^{v}$ for the synthesized derivatives and antifungal activity against *A. flavus* which indicated that compounds **5**, **9** and **13** having high $^{1}\chi^{v}$ values (21.539, 20.928 and 20.951, respectively; Table 2) will have high antifungal potential and the results presented in Table 1 are in concordance with the model expressed by Eq. (1).

The linear regression model expressed by Eq. (1) was subjected to cross validation procedure and high q^2 values ($q^2 = 0.898$) were obtained with leave one out (LOO) method. The foremost requirement for qualifying a statistical model to be a valid one is that it should have q^2 value higher than 0.5, thus supporting the fact that model expressed by Eq. (1) is a valid one (Golbraikh and Tropsha 2002). The comparison of observed and predicted antifungal activities is presented in Table 5, in supplementary materials. The observed and predicted antifungal activities obtained by Eq. 1 lie close to each other as depicted by their low residual values (Table 5), which again supported the validity of model expressed by Eq. (1). The statistical validity of QSAR model was also cross checked by plotting the graphs of observed, predicted and residual pMIC activity values. The plot of predicted $p\mathrm{MIC}_{\mathrm{af}}$ against observed $p\mathrm{MIC}_{\mathrm{af}}$ (Fig. 2, in supplementary materials) also supported the validity of model expressed by Eq. (1). The propagation of error was observed on both sides of zero while plotting the observed $p\mathrm{MIC}_{\mathrm{af}}$ vs residual $p\mathrm{MIC}_{\mathrm{af}}$ (Fig. 3, in supplementary materials), which depicted that there was no systemic error in model development (Kumar et al. 2007; Judge et al. 2012a).

QSAR models represented by Eqs. (2–5) were obtained by linear regression of the antibacterial and antifungal activity of synthesized derivatives against *B. cereus*, *S. aureus*, *P. aeruginosa* and *A. niger* with structural descriptors.

QSAR model for antibacterial activity against *B. cereus*

$$\begin{aligned} &\mathrm{pMIC}_{\mathrm{bc}} = 0.077\,{}^{0}\chi^{\mathrm{v}} + 0.339 \\ &n = 20 \quad r = 0.987 \quad r_2 = 0.974 \quad q_2 = 0.970 \\ &s = 0.054 \quad \mathrm{F} = 676.517 \end{aligned} \tag{2}$$

QSAR model for antibacterial activity against *S. aureus*

$$\begin{aligned} &\mathrm{pMIC}_{\mathrm{sa}} = 0.152\,{}^{2}\chi + 0.057 \\ &n = 20 \quad r = 0.958 \quad r_2 = 0.917 \quad q_2 = 0.902 \\ &s = 0.099 \quad \mathrm{F} = 199.955 \end{aligned} \tag{3}$$

QSAR model for antibacterial activity against *P. aeruginosa*

$$\begin{aligned} &\mathrm{pMIC}_{\mathrm{pa}} = 0.051\,{}^{0}\chi^{\mathrm{v}} + 1.056 \\ &n = 20 \quad r = 0.918 \quad r_2 = 0.842 \quad q_2 = 0.822 \\ &s = 0.095 \quad \mathrm{F} = 96.183 \end{aligned} \tag{4}$$

QSAR model for antifungal activity against *A. niger*

$$\begin{aligned} &\mathrm{pMIC}_{\mathrm{an}} = 0.092\,{}^{2}\chi + 1.079 \\ &n = 20 \quad r = 0.791 \quad r_2 = 0.626 \quad q_2 = 0.575 \\ &s = 0.154 \quad F = 30.114 \end{aligned} \tag{5}$$

The QSAR model for antibacterial activity of synthesized derivatives against *B. cereus* indicated that the antibacterial activity is influenced by the valence zero-order molecular connectivity topological index ($^{0}\chi^{v}$, Eq. 2). The molecular descriptor ($^{0}\chi^{v}$) which governs the antibacterial activity against *B. cereus* pointed towards the unbranched structure of the molecule. The coefficient of

valence zero-order molecular connectivity topological index ($^0\chi^v$) is positive; therefore, the antibacterial activity against *B. cereus* will increase with increase in $^0\chi^v$ values, which can be checked from the results presented in Tables 1 and 2.

The computational model regarding antibacterial activity of the synthesized compounds against *S. aureus* (Eq. 3) indicated that second-order molecular connectivity index ($^2\chi$) was governing the antibacterial activity of synthesized derivatives. The positive coefficient of second-order molecular connectivity index ($^2\chi$) in Eq. (3) revealed that the antibacterial potential of the synthesized derivatives will increase with increase in value of second-order molecular connectivity index ($^2\chi$) which is supported by the results presented in Tables 1 and 2.

The QSAR model for antibacterial activity against *P. aeruginosa* represented by Eq. (4) depicted the role of valence zero-order molecular connectivity indexes ($^0\chi^v$) in altering the antibacterial activity of the synthesized derivatives. The mathematical model represented by Eq. (5) demonstrated the importance of second-order molecular connectivity index ($^2\chi$) in expression of the antifungal activity of synthesized derivatives against *A. niger*. The positive correlation of these molecular descriptors with their respective antibacterial and antifungal activity revealed that increase in the values of structural parameters will lead to an increase in the activity against the respective microorganism. Statistically valid models were not obtained for correlation of antibacterial activity of synthesized derivatives against *E. coli*.

The QSAR models represented by Eqs. (2–5) have got high r, r^2, q^2 and F values and low s values which indicated that the models are valid. The low residual values obtained while predicting the antimicrobial activity using these models (Table 5, in supplementary materials) confirmed the fact that models expressed by Eqs. (2–5) were also valid ones.

Conclusion

The diorganotin(IV) complexes were prepared by reacting sodium salts of 2-amino-6-substituted benzothiazole-derived Schiff bases with dialkyltindichloride(IV). The synthesized complexes have been characterized by different spectroscopic techniques (^{1}H, ^{13}C, ^{119}Sn NMR and IR spectroscopy). The Schiff base ligands were found to be coordinated with tin metal in a bidentate manner (N, O) producing complexes with distorted trigonal bipyramidal geometry and pentacoordinated. The compounds were further evaluated for their in vitro antimicrobial activity against different pathogenic bacteria and fungi. The results of antimicrobial activity indicated that these compounds were highly active against the tested microorganisms and some compounds were equipotent to the standard drugs particularly against *S. aureus* and *A. niger*. The computational analysis revealed that the antimicrobial activity of the synthesized compounds is governed by the molecular connectivity indices including $^0\chi^v$ (valence zero-order molecular connectivity index), $^1\chi^v$ (valence first-order molecular connectivity index), $^2\chi$ (second-order molecular connectivity index) and a detailed view of QSAR analysis indicated that molecules were more potent than the other synthesized compounds and it can be assumed that similar structures having branching around the central metal atom will be highly active.

Acknowledgements The authors are grateful to the Dr. A.P.J. Abdul Kalam-Central Instrumentation Laboratory, Guru Jambheshwar University of Science & Technology, Hisar and Sophisticated Analytical Instrument Facility, Punjab University, Chandigarh for providing IR and NMR facilities. One of the authors, Ms. Aarti Ahlawat is thankful to UGC, New Delhi for providing financial assistance under the Scheme Rajiv Gandhi National Fellowship. The authors are thankful to Dr. Namita Singh, Department of Bio and Nanotechnology, Guru Jambheshwar University of Science and Technology, Hisar for providing bacterial and fungal strains for evaluation of antimicrobial activities.

References

Aman R, Matela G (2013) Tin (IV) complexes of Schiff base derived from amino acid: synthesis and characteristic spectral studies. J Chem 2013:1–4. doi:10.1155/2013/637290

Asija S, Malhotra N, Malhotra R (2012) Bioactive penta-coordinated diorganotin(IV) complexes of Pyridoxalimine Schiff bases. Phosphorus Sulfur Silicon 187:1510–1520. doi:10.1080/10426507.2012.692129

Balaban AT (1982) Highly discriminating distance based topological indices. Chem Phys Lett 89:399–404. doi:10.1016/0009-2614(82)80009-2

Basu S, Masharing C, Das B (2012) Diorganotin(IV) complexes of polyaromatic azo-azomethine ligand from salicylaldehyde and ortho-aminophenol: synthesis, characterization and molecular structure. Heteroatom Chem 23(5):457–465. doi:10.1002/hc.21037

Baul TSB, Masharing C, Basu S, Pettinari C, Rivarola E, Chantrapromma S, Fun HK (2008) Synthesis, characterization of some diorganotin(IV) complexes of Schiff bases derived from a non-protein amino acid. Crystal structures of HO2CC6 H4[N=C(H)}{C(CH3)CH(CH3)–3–OH]-p and its di-n-butyltin(IV) complex (nBu2Sn{O2CC6H4[N=C(H)}{C(CH3) CH(CH3)–3–OH]–p}2). Appl Organometal Chem 22:114–121. doi:10.1002/aoc.1358

Beltran HI, Zea CD, Ortega SH, Camacho AN, Apan MTR (2007) Synthesis and characterization of di-phenyl-tin(IV)-salicyliden-ortho-aminophenols: analysis of in vitro antitumor/antioxidant activities and molecular structures. Inorg Biochem 101:1070–1085. doi:10.1016/j.jinorgbio.2007.04.002

Braunstein P, Morise X (2000) Dehydrogenative coupling of hydrostannanes catalyzed by transition-metal complexes. Chem Rev 100:3541–3552. doi:10.1021/cr000444d

Devi J, Kumari S, Malhotra R (2012) Synthesis, spectroscopic studies, and biological activity of organosilicon(IV) complexes of ligands derived from 2-aminobenzothiazole derivatives and

2-hydroxy-3-methoxy benzaldehyde. Phosphorus Sulfur Silicon 187:587–597. doi:10.1080/10426507.2011.634465
Dias LC, Lima GM, Takahashi JA, Ardisson JD (2015) New di- and triorganotin(IV) carboxylates derived from a Schiff base: synthesis, characterization and in vitro antimicrobial activities. Appl Organometal Chem 29:305–313. doi:10.1002/aoc.3292
Ekennia AC, Onwudiwe DC, Olasunkanmi LO, Osowole AA, Ebenso EE (2015) Synthesis, DFT calculation, and antimicrobial studies of novel Zn(II), Co(II), Cu(II), and Mn(II) heteroleptic complexes containing benzoylacetone and dithiocarbamate. Bioinorg Chem Appl 2015:1–12. doi:10.1155/2015/789063
Elebier MC, Ahin ES, Ancın N, Oztaş NA, Oztas SG (2007) Synthesis and characterization of diorganotin (IV) complexes of Schiff bases with ONO-type donors and crystal structure of [N-(2-hydroxy-4-nitrophenyl)-3-ethoxysalicylideneiminato] diphenyltin (IV). Appl Organometal Chem 21:913–918. doi:10.1002/aoc.1311
Gill RK, Rawal KR, Bariwal J (2015) Recent advances in the chemistry and biology of benzothiazoles. Arch Pharm Chem Life Sci 348:155–178. doi:10.1002/ardp.201400340
Golbraikh A, Tropsha A (2002) Beware of q^2. J Mol Gr Model 20:269–276. doi:10.1016/s1093-3263(01)00123-1
Gonzalez A, Gomez E, Lozada AC, Hernandez S, Apan TR, Comacho AN (2009) Heptacoordinate tin(IV) compounds derived from pyridine Schiff bases: synthesis, characterization, in vitro cytotoxicity, anti-inflammatory and antioxidant activity. Chem Pharm Bull 57(1), 5–15. doi:19122310
Hansch C, Fujita ST (1964) ρ-σ-π analysis. A method for the correlation of biological activity and chemical structure. J Am Chem Soc 86:1616–1626. doi:10.1021/ja010629035
Hansch C, Leo A, Unger SH, Kim KH, Nikaitani D, Lien EJ (1973) Aromatic substituent constants for structure-activity correlations. J Med Chem 16(11):1207–1216. doi:10.1021/jm00269a003
Hong M, Yin HD, Chen SW, Wang DQ (2010) Synthesis and structural characterization of organotin(IV) compounds derived from the self-assembly of hydrazone Schiff base series and various alkyltin salts. J Organomet Chem 695:653–662. doi:10.1016/j.jorganchem.2009.11.035
Hyperchem 6.0, Hypercube Inc (1993) Florida
Judge V, Narasimhan B, Ahuja M, Sriram D, Yogeeswari P, De Clercq E, Pannecouque C, Balzarini J (2012a) Isonicotinic acid hydrazide derivatives: synthesis, antimicrobial activity and QSAR studies. Med Chem Res 21(7):1451–1470. doi:10.1007/s00044-011-9662-9
Judge V, Narasimhan B, Ahuja M, Sriram D, Yogeeswari P, De Clercq E, Pannecouque C, Balzarini J (2012b) Synthesis, antimycobacterial, antiviral, antimicrobial activity and QSAR studies of isonicotinic acid-1-(substituted phenyl)-ethylidene/cycloheptylidene hydrazides. Med Chem Res 21(8):1935–1952. doi:10.1007/s00044-011-9705-2
Kashar TI (2014) Synthesis, characterization and biological activity of some metal complexes of benzoylacetone Schiff base. Eur Chem Bull 3(9), 878–882. doi:02200/02286/00031
Kemmer M, Dalil H, Biesmans M (2000) Dibutyltin perfluoroalkanecarboxylates: synthesis, NMR characterization and in vitro antitumour activity. J Organomet Chem 608:63–70. doi:10.1016/S0022-328X(00)00367-3
Kier LB, Hall LH (1976) Molecular connectivity in chemistry and drug research. Academic Press, NewYork. doi:10.1002/jps.2600660852
Kumar A, Narasimhan B, Kumar D (2007) Synthesis, antimicrobial and QSAR studies of substituted benzamides. Bioorg Med Chem 15:4113–4124. doi:10.1016/j.bmc.2007.03.074
Lather V, Madan AK (2005) Topological models for the prediction of anti-HIV activity of dihydro(alkylthio) (naphthylmethyl) oxopyrimidines. Bioorg Med Chem 13, 1599–1604. http://www.ncbi.nlm.nih.gov/labs/article/15698777/
Mene D, Kale M (2016) Exploration of different methodologies for synthesizing biologically important benzothiazoles: an overview. Curr Org Synth 13(1):41–57. doi:10.2174/1570179412999150723154128
Mohammadi K, Zahedi M (2012) Tridentateschiff base compounds of 2-aminophenol: synthesis, characterization and complexation with IIIA elements. Global J Inorg Chem 3(2), 1-12. doi:103637225
Mun LS, Hapipah MA, Shin SK, Nurestrib AMS, Mun LK (2012) "Synthesis, structural characterization and in vitro cytotoxicity of diorganotin complexes with Schiff base ligands derived from 3-hydroxy-2-naphthoylhydrazide. Appl Organometal Chem 26:310–319. doi:10.1002/aoc.2862
Nath M, Yadav R, Gielen M, Dalil H, Vos D, Eng G (1997) Synthesis, characteristic spectral studies and in vitro antimicrobial and antitumour activities of organotin(IV) complexes of Schiff bases derived from amino-acids. Appl Organometal Chem 11:727–736. doi:10.1002/(SICI)1099-0739(199709)11:9<727:AID-AOC639>3.0.CO;2-X
Nath M, Saini PK, Kumar A (2009) Synthesis, structural characterization, biological activity and thermal study of tri and diorganotin (IV) complexes of Schiff base derived from 2-aminomethylbenzimidazole. Appl Organometal Chem 23:434–445. doi:10.1002/aoc.1537
Nidhi Sonika, Malhotra R (2011) Synthesis and characterization of diorganotin(IV) complexes with tridentate Schiff base ligand pyridoxal aroylhydrazones. Phosphorus Sulfur Silicon 186:1449–1459. doi:10.1080/10426507.2010.517583
Randic M (1975) Characterization of molecular branching. J Am Chem Soc 97:6609–6615. doi:10.1021/ja00856a001
Randic M (1993) Comparative regression analysis: regression based on a single descriptor. Croat Chem Acta 66, 289–312. url:hrcak.srce.hr/137063
Sallam SA, Orabi AS (2002) Copper, nickel and cobalt complexes of Schiff-bases derived from β-diketones. Transit Metal Chem 27:447–453. doi:10.1023/A:1015085023602
Sedaghat T, Shokohi-pour Z (2009) Synthesis and spectroscopic studies of new organotin(IV) complexes with tridentate N- and O-donor Schiff bases. J Coord Chem 62(3):3837–3844. doi:10.1080/00958970903180103
Sharma P, Rane N, Gurram VK (2004) Synthesis and QSAR studies of pyrimido[4,5-d]pyrimidine-2,5-dione derivatives as potential antimicrobial agents. Bioorg Med Chem Lett 14:4185. doi:10.1016/j.bmcl.2004.06.014
Sharma A, Jain A, Saxena S (2015) The structure–activity relationship of some hexacoordinated dimethyltin(IV) complexes of fluorinated β-diketone/β-diketones and sterically congested heterocyclic β-diketones. Appl Organometal Chem 29(8):499–508. doi:10.1002/aoc.3321
Sharma C, Bansal PK, Kushal Aakash D, Pathak Meenakshi (2017) Benzothiazole derivatives as potential anti-infective agents. Curr Top Med Chem 17(2):208–237. doi:10.2174/1568026616666160530152546
Silva CM, Silva DL, Modolo LV, Alves RB, Resende MA, Martins CVB, Fatima AD (2011) Schiff bases: a short review of their antimicrobial activities. J Adv Res 2:1–8. doi:10.1016/j.jare.2010.05.004
Singh K, Kumar Y, Pundir RK (2010) Synthesis and characterization of biologically active organosilicon (IV) complexes with Schiff bases derived from o-aminothiophenol. Synth React Inorg Metal-org Nano-Met Chem 40:836–842. doi:10.1080/15533174.2010.522646
Sonika Narula AK, Vermani OP, Sharma HK, Sarpal AS (1994) Synthesis of bimetallic [Sn(IV), Al(III)]-μ-oxoisopropoxyacetate and bimetallic [Sn(IV), Al(III)]-μ-oxoisopropoxide and their acetylacetone and benzoylacetone derivatives. J Organometal Chem 470(1–2):67–72. doi:10.1016/0022-328x(94)80149-5

Spooner DF, Sykes G (1972) Methods in microbiology. Academic Press, London

SPSS for Windows, version 10.05, SPSS Inc (1999) Bangalore, India

TSAR 3D Version 3.3 (2000) Oxford Molecular Limited

Wiener H (1947) Structural determination of paraffin boiling points. J Am Chem Soc 69:17–20. doi:10.1021/ja011939005

Yenisehirli G, Oztas NA, Sahin E, Celebier M, Ancın N, Oztas SG (2010) Synthesis, characterization, and in vitro antimicrobial activities of organotin (IV) complexes of Schiff bases with ONO-type donor atoms. Heteroatom Chem 21(6):373–385. doi:10.1002/hc.20628/pdf

Yin HD, Chen SW (2006) Synthesis and characterization of di- and tri-organotin(IV) complexes with Schiff base ligand pyruvic acid 3-hydroxy-2-naphthoyl hydrazone. Inorg Chim Acta 359:3330–3338. doi:10.1016/j.ica.2006.03.024

Yin HD, Ganghi MH, Wang DQ (2005) Synthesis, characterization and structural studies of diorganotin(IV) complexes with Schiff base ligand salicylaldehyde and isonicotinylhydrazone. J Organomet Chem 690:3714–3719. doi:10.1016/j.jorganchem.2005.04.049